ISTITUTO NAZIONALE DI FISICA NUCLEARE

Sezione di Napoli

INFN/TC-98/26
26 Ottobre 1998

NONLINEAR FLUID EFFECTS ON THE LONGITUDINAL INSTABILITIES OF COASTING BEAMS

I. Hofmann, G. Miano, G. Rumolo, C. Serpico

SIS–Pubblicazioni
dei Laboratori Nazionali di Frascati

Istituto Nazionale di Fisica Nucleare
Sezione di Napoli

INFN/TC-98/26
26 Ottobre 1998

NONLINEAR FLUID EFFECTS ON THE LONGITUDINAL INSTABILITIES OF COASTING BEAMS

I. Hofmann [1], G. Miano [2,3], G. Rumolo [1,2,3], C. Serpico [2]

[1] GSI, Planckstr. 1, 64291 Darmstadt, Germany
[2] Dipartimento d'Ingegneria Elettrica, Università degli Studi di Napoli Federico II, Via Claudio 21, 80125 Napoli, Italy
[3] INFN–Sezione di Napoli, Dipartimento di scienze fisiche, Via Cintia, Montesantangelo, 80125 Napoli, Italy

Abstract

A simple nonlinear cold fluid model of a coasting beam is used to explain the generation of higher order harmonics and steepening of line charge density spatial profiles observed during the development of longitudinal instabilities in the ESR far beyond the stability boundary. The storage ring operates with high currents and below the transition energy. For different values of the machine impedance the cold fluid model is solved and the results are compared with the particle-in-cell simulations obtained by using SCOP-RZ/PATRIC code as well as with the measurements made at the ESR in 1997. The harmonic generation in the early stage of the instability nonlinear phase and the consequent asymmetric steepening of the density profile are due to the fact that different values of the line charge density wave "propagate" backward with different velocities: higher values propagate faster than lower ones. This is a nonlinear convective effect well known in gas and fluid dynamics. The limits of the applicability of the cold fluid model have been also pointed out.

1. Introduction

The study of coherent longitudinal instabilities of particle coasting beams in accelerators and storage rings, caused by the interaction with self-induced electromagnetic fields, has received recently new attention in connection with the research on high-current circular machines operating below transition energy [1]. So far, a wide theoretical investigation of the linear phase of the instabilities has been made through a linearized kinetic model [2]. The nonlinear stages of the longitudinal instability evolution for a coasting beam operating above the transition energy have been seldom taken into consideration and the attention has been in general mostly concentrated on the formation of clusters of charges [3], saturation, decoherence effects [4] and on the overshoot

of the momentum spread of the beam [5], [6]. The possibility of the existence of finite amplitude waves exhibiting steepening and solitons has pointed out in [7] and [8] by using a heuristic cold fluid model in which relativistic and revolution frequency dispersion effects are disregarded: an intense coasting beam below the transition energy is considered and only the effects of the space charge are examined closely. In general the form of the machine impedance is important for determining whether such phenomena may exist.

The aim of the present paper is to give a simple physical explanation of some observed nonlinear phenomena in the ESR measurements such as the formation of a shock wave, its subsequent breaking and saturation and the generation of higher order harmonics [9],[10]. The ESR storage ring is a high-current machine operating below transition energy. During the measurements the machine was operating far outside the stability boundary. The longitudinal impedance of the machine consists of the space charge impedance and the impedance of the resonant cavity that during the measurements was tuned near the beam revolution frequency.

It is well known that far outside the stability boundary a linear cold fluid model (*e.g.*, [11]) predicts very well the frequency shift and the grow time of the instability both qualitatively and quantitatively. This suggests us that some of the observed nonlinear phenomena at ESR may be due to collective nonlinear fluid effects such as the convection. In this paper the early stage of the nonlinear phase of the longitudinal instabilities in the ESR are investigated by using a nonlinear cold fluid model for different values of the longitudinal impedance.

We derive from the kinetic equation for the longitudinal motion a macroscopic cold fluid model by using the technique of the moments: we take into account the relativistic effects and the effects due to the dispersion of the revolution beam frequency to the leading order. In this model the nonlinearity only arises from the convective phenomenon. We find an analytical solution of the cold fluid equations in the one case when this is possible, namely when considering a beam below transition that interacts with a purely space charge impedance (a stable beam), whereas for the more interesting unstable case numerical solutions have come to be necessary. The results obtained by using the cold fluid model are compared with the particle-in-cell PATRIC simulations [9] and with the measured data from the ESR [10] so that it becomes clear how far the macroscopic cold fluid model provides a correct description of the beam dynamics and what nonlinear effects it is able to fully explain.

2. Review of the kinetic model

Since 1981 Bisognano *et all* proposed a cold fluid model in which the longitudinal electric field acting on the beam is due to the space charge and the resistive wall effects. Relativistic and revolution frequency dispersion effects are disregarded. Here we will derive a cold fluid model taking into account, in a self-consistent way, the relativistic and revolution frequency dispersion effects for an arbitrary longitudinal impedance of the machine. This is accomplished by applying the technique of the moments to the kinetic equation describing the longitudinal motion of the particle beam in presence of any longitudinal impedance.

Let us consider a coasting beam moving in a circular machine, (*i.e.*, a storage ring or a circular accelerator), with nominal longitudinal velocity U_0 and nominal circular "equilibrium" orbits with radius r_0; $C_0 = 2\pi r_0$ is the circumference length. In the following we will always use the symbols θ and r for the azimuthal and radial co-ordinates, respectively. Furthermore, with ω and ε we will indicate the angular frequency, $\omega = \dot{\theta}$, and the total energy of the particle;

$\omega_0 = U_0 / r_0$ is the nominal angular frequency. The radius of the equilibrium orbit of the particle depends on the angular frequency, $r = r(\omega)$, according to the momentum compaction and slip factors, and the revolution frequency of the generic particle depends on its energy ε, according to the frequency dispersion of the ring $\omega = \omega(\varepsilon)$, (*e.g.*, [11]).

We start describing the beam by means of the distribution function $g(\theta, w; t)$ in the phase space (θ, w) where w is defined as

$$w(\varepsilon) \triangleq 2\pi \int_{\varepsilon_0}^{\varepsilon} \frac{d\varepsilon}{\omega(\varepsilon)}. \tag{1}$$

Let us suppose that the longitudinal component $E = E(\theta, r; t)$ of the electric field acting on the particles (due to the space charge and to the interaction of the beam with the surroundings) depends on the radial co-ordinate r as $1/r$,

$$E(r, \theta; t) = -\frac{\phi(\theta; t)}{2\pi r}, \tag{2}$$

where the "potential" function $\phi(\theta; t)$ is independent to the particle radius. Under this assumption θ and w are conjugate variables. An immediate consequence of this property is that the distribution function $g(\theta, w; t)$ is solution of the kinetic equation

$$\frac{\partial g}{\partial t} + \omega(w)\frac{\partial g}{\partial \theta} - q\phi(\theta; t)\frac{\partial g}{\partial w} = 0, \tag{3}$$

where q is the electric charge of the particle. We have neglected collision phenomena because they do not play a considerable role on the time scale of the instability we are interested in (this assumption may be always checked "a posteriori"). In this model the electric field E is the averaged field over small phase space volumes so as to be cleaned out of the fluctuations due to the microscopic discrete nature of the particle beam.

To derive the cold fluid model we need the kinetic description of the beam in the velocity phase space. Let us introduce the two independent variables s and u

$$\begin{aligned} s &= r_0\theta, \\ u &= r_0 v, \end{aligned} \tag{4}$$

and let be $f(s, u; t)$ the distribution function of the beam in the phase space (s, u) (the spatial co-ordinate s is defined on the interval $(0, C_0)$). The distribution function $f(s, u; t)$ is related to the distribution function $g(\theta, w; t)$ through the relation

$$f(s, u, t) = \frac{1}{r_0^2}\left|\frac{dw}{d\omega}\right| g(\theta, w, t). \tag{5}$$

Assuming a small relative energy spread of the beam particles, we may replace ω by its nominal mean value ω_0 in the integral (1) and we may linearize the dispersion relation that links the angular frequency to the particle energy,

$$\omega(\Delta\varepsilon) = \omega_0 + \kappa_0 \Delta\varepsilon, \tag{6}$$

where $\Delta\varepsilon \triangleq \varepsilon - \varepsilon_0$, $\kappa_0 \triangleq -\eta\omega_0 / (\beta_0^2 \varepsilon_0)$, $\beta_0 = U_0 / c$, $\varepsilon_0 = m_0 c^2 \gamma_0$, η is the frequency slip factor, m_0 is the rest mass of the particles and $\gamma_0 = (1 - \beta_0^2)^{-1/2}$. By using these approximations we obtain for the leading term

$$w(\varepsilon) \cong 2\pi(\varepsilon - \varepsilon_0)/\omega_0, \tag{7}$$

and

$$f(s,u;t) \cong \frac{2\pi}{r_0^2|\kappa_0|\omega_0} g(\theta,w;t). \tag{8}$$

Therefore the distribution function $f(s,u;t)$ is solution of the Vlasov equation

$$\frac{\partial f}{\partial t} + u\frac{\partial f}{\partial s} - \frac{q}{m^*}\frac{\phi(s;t)}{2\pi r_0}\frac{\partial f}{\partial u} = 0. \tag{9}$$

To derive the equation (9) we have used the relation

$$\frac{\omega_0 r_0}{\beta_0^2 \varepsilon_0} = \frac{U_0}{\beta_0^2 \varepsilon_0} = \frac{1}{p_0}, \tag{10}$$

where p_0 is the nominal momentum of the beam particle. Furthermore, we have introduced the "effective" particle mass

$$m^* = -\frac{p_0}{U_0 \eta}. \tag{11}$$

Note that below transition m^* is positive.

Finally we have to specify the form of the driving term ϕ present in the Vlasov equation (9). In general $\phi(t)$ is made up of two different contributions: an external voltage acting on the beam, which can represent either a bunching field oscillating in the RF cavity or a residual field detuned with respect to the beam revolution frequency, and a self-voltage coming from the interaction of the beam with the beam itself and with the surrounding environment.

It is possible in our case to represent the latter on the spatial m^{th} harmonic as the product of the beam current component at that harmonic times the coupling longitudinal impedance at the same harmonic, which synthetically describes all the mentioned interactions of the beam at that harmonic number. Thus the electric "potential" $\phi(s,t)$ is linked to the beam electric current intensity

$$I(s,t) = q\int_{-\infty}^{+\infty} uf(s,u,t)du, \tag{12}$$

through the relation

$$\phi(s,t) = \sum_m \dot{Z}(m\omega_0) I_m(t) e^{-imk_0 s} + \phi_{ext}(s,t), \tag{13}$$

where $k_0 = (\omega_0/u_0) = 1/r_0$,

$$I_m(t) = \frac{1}{C_0}\int_0^{C_0} I(s,t) e^{imk_0 s} ds, \tag{14}$$

$\dot{Z} = \dot{Z}(\omega)$ is the total longitudinal impedance of the machine and $\phi_{ext}(s,t)$ is an applied forcing term, *i.e.*, it takes into account the action of an RF cavity. Using the value of the impedance estimated exactly at $\omega = m\omega_0$ is in fact an approximation, since the time dependence of the beam current signal makes it not purely oscillating at the multiples of the revolution frequency but at shifted values. However, in our case the frequency shift at the operating mode, which is of the order of 10 Hz, is small compared to the characteristic band of the environment impedance (of the order of 10 kHz) and thus we can neglect this effect.

3. Nonlinear cold fluid model

In order to deduce from the kinetic model the equations for the dynamics of the macroscopic fluid quantities characterising the beam, such as the distribution of its line density, the mean velocity and the current intensity along the ring, we have to calculate the momenta of Vlasov equation (9) by multiplying it with powers of the velocity u and integrating over the velocity space. With this regard, we firstly remind how the numeric line density of the beam $n(s,t)$ and and the mean velocity $U(s,t)$ are related to the distribution function f,

$$\begin{aligned} n(s,t) &\triangleq \int_{-\infty}^{\infty} f(s,u,t)du, \\ U(s,t) &\triangleq \frac{\int_{-\infty}^{\infty} uf(s,u,t)du}{n(s,t)}. \end{aligned} \tag{15}$$

For the beam current intensity $I(s,t)$ we have

$$I(s,t) = qn(s,t)U(s,t) \cong qU_0 n(s,t). \tag{16}$$

In equation (16) we have approximated the actual averaged velocity of the beam with the nominal mean velocity U_0 because in our case the shift of the actual mean velocity from the nominal one is very small compared with U_0.

Let us start with the zero-order moment obtained by multiplying by $u^0 = 1$ and integrating on the velocity space. The first term of equation (9) becomes

$$\left\langle \frac{\partial f}{\partial t} \right\rangle = \frac{\partial n}{\partial t}, \tag{17}$$

the second

$$\left\langle u\frac{\partial f}{\partial s} \right\rangle = \frac{\partial}{\partial s}(nU), \tag{18}$$

and the third

$$-\frac{q}{m^*}\frac{\phi(s,t)}{2\pi r_0 p_0}\left\langle \frac{\partial f}{\partial u} \right\rangle = -\frac{q}{m^*}\frac{\phi(s,t)}{2\pi r_0 p_0}\left[f(s,u,t)\right]_{u=-\infty}^{u=\infty} = 0, \tag{19}$$

where the symbol $\langle f \rangle$ indicates $\int_{-\infty}^{+\infty} f du$. Since no particles can have infinite velocity, f falls very rapidly as $u \to \pm\infty$. By using the expressions (17)-(19), from equation (9) we have the continuity equation in the configuration space s

$$\frac{\partial n}{\partial t} + \frac{\partial}{\partial s}(nU) = 0. \tag{20}$$

If we multiply now equation (9) by u and then integrate it on the velocity space, the first term becomes:

$$\left\langle u\frac{\partial f}{\partial t} \right\rangle = \frac{\partial}{\partial t}\langle nU \rangle, \tag{21}$$

the second

$$\langle u^2 \frac{\partial f}{\partial s} \rangle = \frac{\partial}{\partial s}\left(nU^2\right) + \frac{\partial}{\partial s}\left\langle (u-U)^2 f \right\rangle, \tag{22}$$

and the third

$$-\frac{q}{m^*}\frac{\phi}{2\pi r_0}\langle u \frac{\partial f}{\partial u} \rangle = \frac{q}{m^*}\frac{n\phi}{2\pi r_0}. \tag{23}$$

In this way we get the equation of the "momentum" conservation

$$\frac{\partial}{\partial t}(m^* nU) + \frac{\partial}{\partial s}\left[\left(m^* nU\right)U + \Pi\right] = -q\frac{n\phi}{2\pi r_0}, \tag{24}$$

where the new "macroscopic" quantity $\Pi(s,t)$ given by

$$\Pi(s,t) = \left\langle m^*(u-U)^2 f \right\rangle, \tag{25}$$

takes into account the effects due to the spread in the longitudinal velocity of the particle beam. The quantities $P(s,t) = m^* n(s,t)U(s,t)$ and $\Pi(s,t)$ may be considered, respectively, as the longitudinal line momentum density and the longitudinal "kinetic pressure" of the beam. The pressure contribution in (24) may be interpreted as the additional momentum flux due to the particle motion relative to the mean one.

In this paper we will study the nonlinear fluid effects on the longitudinal instabilities of a coasting beam in the cold fluid limit $\Pi \to 0$. Therefore the system of partial differential equations describing the longitudinal motion of a coasting beam in the cold fluid limit is

$$\begin{cases} \dfrac{\partial \lambda}{\partial t} + \dfrac{\partial}{\partial s}(\lambda U) = 0, \\ \dfrac{\partial U}{\partial t} + U\dfrac{\partial U}{\partial s} = -\dfrac{q}{2\pi r_0 m^*}\phi(s,t). \end{cases} \tag{26}$$

where $\lambda(s,t) = qn(s,t)$ is the linear charge density distribution along the ring. It is useful to reformulate the fluid equations (26) in such a way to hide the "fast" component of the dynamics, that is, the one due to the beam revolution around the ring - its characteristic time being $2\pi/\omega_0$ - and provide the only "slow" components of the beam evolution. For this purpose we perform the following linear transformation of variables:

$$\begin{cases} U = U_0 + V, \\ s = U_0 t + x. \end{cases} \tag{27}$$

By applying this transformation to the system (26) we obtain

$$\begin{cases} \dfrac{\partial \Lambda}{\partial t} + \dfrac{\partial}{\partial x}(\Lambda V) = 0, \\ \dfrac{\partial V}{\partial t} + V\dfrac{\partial V}{\partial x} = -\dfrac{q}{m^*}\dfrac{\psi(x,t)}{2\pi r_0}, \end{cases} \tag{28}$$

where $\Lambda(x,t) = \lambda(x + U_0 t, t)$, $V(x,t) = U(x + V_0 t, t) - U_0$ and $\psi(x,t)$ is given by

$$\psi(x,t) = U_0 \sum_m \dot{Z}(mv_0)\Lambda_m(t)e^{-imk_0 x}, \tag{29}$$

where

$$\Lambda_m(t) = \frac{1}{C_0} \int_0^{C_0} \Lambda(x,t) e^{imk_0 x} dx. \tag{30}$$

The equations (28) have to be solved with the periodic boundary conditions

$$\begin{cases} \Lambda(x=0,t) = \Lambda(x=C_0,t), \\ V(x=0,t) = V(x=C_0,t), \end{cases} \tag{31}$$

and given initial conditions.

4. Machine impedance

The right hand side of the momentum equation is given by equation (12). The potential $\phi(t)$, and hence ψ, depends only on the total impedance of the machine $\dot{Z}$, on the applied RF voltage and on the beam linear charge density $\Lambda(x,t)$. Therefore ψ is completely determined in the cold fluid model.

The impedance consists of the space charge impedance of the beam itself and the impedance of the surroundings. In the case of the ESR the total impedance acting on the beam has a real part, which is mainly the resistive part of the cavity impedance, and an imaginary part, which is given by the sum of the imaginary part of the cavity impedance and the space charge reactance from the beam itself. Thus the generic impedance $\dot{Z}(m\omega_0)$ may be represented as

$$\dot{Z}(m\omega_0) = \dot{Z}_m^{(sc)} + \dot{Z}_m^{(cav)}, \tag{32}$$

where [8]

$$\dot{Z}_m^{(sc)} = -i\xi(m) X_{sc} = -i \frac{m}{1+\alpha^2 m^2} X_{sc}, \tag{33}$$

and

$$\dot{Z}_m^{(cav)} = \frac{R_s}{1 + iQ\left(\frac{m\omega_0}{\omega_c} - \frac{\omega_c}{m\omega_0}\right)}. \tag{34}$$

The space charge reactance X_{sc} does not depend on the wave number m; the order of magnitude of the dimensionless parameter α is given by $\alpha \approx \frac{r_b}{2r_0}\sqrt{[1+2ln(r_p/r_b)]}$ where r_b and r_p are, respectively, the beam and the pipe radii [8]. Therefore, the space charge impedance is proportional to the harmonic number m in the low "frequency" range and then rapidly vanishes when the harmonic number comes closer to $1/\alpha$ due to the image charges on the inner side of the beam pipe. Since for the ESR we have $\alpha \approx 10^{-3}$, the space charge impedance moves away from the ideal expression $-imX_{sc}$ for $m \geq 10^3$. In the ESR measurements harmonics up the 20th have been detected [10], thus one can reasonable assume $\alpha = 0$. In the relation (34) R_s, Q and ω_c are, respectively, the shunt resistance, the quality factor and the fundamental eigenfrequency of the RF cavity.

Since the cavity is tuned near a multiple of the beam revolution frequency, the external voltage can be written as $\phi_{ext}(s,t) = \Phi\cos[m_r(\omega_0 t - k_0 s) - \Delta\Omega t]$, where $\Delta\Omega = m_r\omega_0 - \omega_c$ and Φ is the amplitude. In this paper we analyse the situation where no external voltage is acting on

the beam, and the only electromagnetic force that determines the beam evolution is due to the space charge and the beam-environment interactions.

5. Study of the longitudinal coasting beam instabilities in the ESR

The system of partial differential equations (28) is strongly nonlinear due to the presence of convective terms $\partial(\Lambda V)/\partial x$ and $V(\partial V/\partial x)$. These are the only nonlinearities present in the model since the interaction with the beam itself and with the surrounding environment is of linear type. It is possible, of course, to linearize the system (28) and verify that it predicts a longitudinal exponential instability to occur whenever the impedance is not purely capacitive. Beam stability in case of interaction with an impedance having a resistive part is never possible in this model, because we are neglecting the wave-particle interaction and hence the stabilizing mechanism due to the Landau damping. However the results obtained from the fluid model are to some extent correct if the operating point on the stability diagram is far away from the stability boundary, as in the recent ESR measurements [10].

Table I

E_{kin}	340 MeV/U
γ	1.36
$\nu_0/2\pi$	1.886633 MHz
r_0	17.22 m
η	−0.367
X_{sc}	670 Ω
R_s	1300 Ω
Q	50

In this Section we will use the cold fluid model to examine the longitudinal instabilities in the ESR. Unfortunately the case when the beam is unstable cannot be investigated analytically. In fact the presence of a real part in the impedance makes impossible to carry out the same analytical procedure that we will use in the next Section to study a stable coasting beam below transition interacting with a purely capacitive impedance. Thus a numerical solution of the cold fluid equations is needed.

We solve the cold fluid equations with the parameters of the measurements made at the ESR in February 1997 on a very intense and very cold C^{6+} ion beam ($\left(\Delta p/p_0\right)_{FWHM} = 1.1\cdot 10^5$ and of the relative PATRIC simulations [10]. The complete list of the these parameters is given in Table I. The measurements were done at different values of the beam current. The cavity was tuned near the beam revolution frequency. When the resonance frequency of the cavity is varied in an opportune neighbourhood of the beam revolution frequency, the impedance working point on the longitudinal stability diagrams changes its position and allows investigating the beam dynamics (both linear and nonlinear) in different operating conditions [10].

Three different cases will be studied in the following and then compared with the results from measurements and simulations: the situations they represent correspond to three values of the offset $\Delta f \triangleq (\omega_0 - \omega_c)/2\pi$ between the revolution frequency of the beam and the cavity

eigenfrequency, that are $\Delta f = -17.4\ kHz$, $\Delta f = 0$ and $\Delta f = 16.4\ kHz$. The numerical solution of equations (28) is based on the finite difference approximation of the partial derivative operators. The equations are firstly approximated in space by using the method of the central differences (the error vanishes like Δx^2 for $\Delta x \to 0$, where Δx is the width of the spatial grid). The spatial interval $(0, C_0)$ has been partitioned uniformly in N intervals of width $\Delta x = C_0/N$. At the boundary grid points the conditions (30) coming from the periodicity of the structure are imposed. In all the simulations we have partitioned the ring circumference up to 200 intervals. The Fourier integrals (30) have been evaluated by using the FFT algorithm. The resulting system of ordinary differential equations in time has been then numerically integrated by a fourth order Runge-Kutta algorithm (the corresponding error vanishes like Δt^4 for $\Delta t \to 0$). The time step Δt has been chosen in such a way to assure the stability of the numerical algorithm and to resolve correctly the beam dynamics. The linear theory predicts in all the considered case a frequency shift of the order of 10 Hz. Therefore in all the simulations we have chosen a time step of 1 ms that assures also the stability of the numerical algorithm.

The time integration has been performed by using the initial conditions $V(x, t=0) = 0$ and $\Lambda(x, t=0) = \Lambda_0 + \Lambda_1 \sin(k_0 x)$ with $\Lambda_1 = 6 \cdot 10^{-4} \Lambda_0$. Since $(\Lambda_1 / \Lambda_0) << 1$, we don't need to care about giving initial conditions that meet a special constraint between density and velocity. This is because, although initially both the slow and the fast waves get excited, after a while we are practically left with the only unstable backward wave that grows exponentially in amplitude while the forward one gets damped at the same time. Furthermore the initial density need not be rigorously only on the 1st harmonic, since the narrow band cavity impedance around f_0 causes the only perturbation with $m = 1$ to grow while all the others, if present, would remain stable and thus on the initial level (that can be generally noise level).

The results of the simulations of the cold fluid model show us clearly a dynamic that is the same as the one obtained with the PATRIC code both in the linear phase and in the early nonlinear phase. In figures 1, 2 and 3 the space-time evolution of the line charge density is shown for $\Delta f = -17.4$ kHz, $\Delta f = 0$ and $\Delta f = 16.4$ kHz, respectively, and for a beam current of 0.366 mA. A slow wave growing in amplitude and getting steep towards the left side in the late phase of the instability is clearly observable. Moreover one can see that the wave gets faster the higher is Δf; this is coherent with what one can deduce from the stability diagrams relative to these cases, since the working point shifts upwards when Δf increases.

In Figures 4 we show in detail the line charge density distribution at different phases of the beam evolution for $\Delta f = -17.4$ kHz: at t=160 ms the line density profile is still sinusoidal; at t=280 ms the amplitude is grown and the wave becomes strongly asymmetric with a sharp left edge, till the formation of a strongly depleted zone at t=315 ms. In Figure 5 the time evolution of first, second and third spatial harmonic of the line charge density for $\Delta f = -17.4$ kHz are plotted. They let us clearly deduce the existence of an exponential growing phase already observed with the PATRIC code and predicted theoretically with the linear theory (at least for the first harmonic). The *e-folding* time one could extrapolate fits very well to the theoretical and simulated ones. The rising of second and third harmonic, which we find identical in the PATRIC simulation for the same case [9], is peculiar because we started from a purely sinusoidal perturbation on the fundamental mode with zero higher order harmonics (in the PIC simulation we had anyway an initial condition of Schottky noise that has a contribution, even small but different from zero, on each harmonic number). This is nothing else that a nonlinear effect due to the convective nonlinear terms, which

generate harmonics and hence produce the distortion of the line density profile. A shock wave in the distribution of the mean velocities along the beam is also observable, as we can see in Figure 6. If we compare shapes and peak values of the line densities obtained by using the fluid model with those measured at the ESR before the saturation occurs and with those simulated with the PATRIC code at the same time instants in the instability development ($\Delta f = -17.4$ kHz and beam current of 0.276 mA) an impressive agreement is found out to exist (Figure 7). Unfortunately the saturation in the instability evolution simply doesn't occur in the cold fluid model: the line density peak keeps going up as long as the beam is not completely bunched (see figure 3 at t=315 ms). In other words, the instability goes on until a region of complete particle depletion is created. This is neither in agreement with the PATRIC simulations nor with the measured bunch shapes during a self-bunching process [9-10], which clearly show how a longitudinal instability doesn't lead to a completely self-bunched beam in the end but stops somewhere before. For the same case, Figure 8 shows the 1st harmonic time evolution extrapolated from the cold fluid solution, along with the ones coming from the measured data and the corresponding PATRIC simulation. We realize that the instability predicted by the fluid model is a bit faster, but this is easily understandable if we consider that in the fluid model the Landau damping effect is absent. Furthermore, the saturation that appears clearly both in the experimental points and in the PIC simulation is on the contrary completely absent in the fluid evolution.

6. Analysis of the asymmetric steepening phenomenon

In order to understand deeply the mechanism at the basis of the asymmetric steepening phenomenon, in this Section we consider a particular significant case that can be analytically investigated.

An analytical solution of the nonlinear equations (28) can be found if one consider a beam interacting with an impedance purely capacitive proportional to the harmonic number, *i.e.*, $\alpha = 0$ in expression (32). In this case the beam is stable. Thus we obtain for the potential ψ:

$$\psi(x,t) = U_0 X_{sc} \sum_m [-im\Lambda_m(t) e^{-imk_0 x}] = \frac{U_0 X_{sc}}{k_0} \frac{\partial \Lambda}{\partial x}, \tag{35}$$

where $\Lambda_m(t)$ is the m-th Fourier component of the line charge density $\Lambda(x,t)$. Then the system (28) becomes

$$\begin{cases} \dfrac{\partial \Lambda}{\partial t} + \dfrac{\partial}{\partial x}(\Lambda V) = 0, \\ \dfrac{\partial V}{\partial t} + V \dfrac{\partial V}{\partial x} + \chi \dfrac{\partial \Lambda}{\partial x} = 0, \end{cases} \tag{36}$$

where the coefficient χ has been defined as

$$\chi \triangleq -\frac{\eta}{p_0} \frac{v_0}{2\pi} \frac{qU_0 X_{sc}}{k_0}. \tag{37}$$

The parameter χ is positive definite if the particle beam is below the transition energy, $\eta < 0$, whereas it is negative above the transition energy $\eta > 0$. Here we consider only the case $\eta < 0$ for which the analytical solution exists.

The linearization of this system under the assumption of small perturbations, *i.e.*,

$\Lambda(x,t) = \Lambda_0 + \delta\Lambda(x,t)$, $V(x,t) = \delta V(x,t)$ (the coasting beam equilibrium is characterized by the uniform line charge density Λ_0 and by a zero mean velocity in the frame defined by the transformations (27)), leads to:

$$\begin{cases} \dfrac{\partial \delta\lambda\Lambda}{\partial t} + \Lambda_0 \dfrac{\partial \delta V}{\partial x} = 0, \\ \dfrac{\partial \delta V}{\partial t} + \chi \dfrac{\partial \delta\Lambda}{\partial x} = 0. \end{cases} \tag{38}$$

It is quite easy to prove that the general solution of this couple of equations is a combinations of forward and backward waves of the type

$$\begin{aligned} \delta\Lambda(x,t) &= F_-(x - c_s t) + F_+(x + c_s t), \\ \delta V(x,t) &= G_-(x - c_s t) - G_+(x + c_s t), \end{aligned} \tag{39}$$

where the propagation velocity of the waves is given by

$$c_0 = \sqrt{\Lambda_0 \chi}, \tag{40}$$

and

$$G_- = \frac{c_s}{\Lambda_0} F_-, \quad G_+ = -\frac{c_s}{\Lambda_0} F_+ \tag{41}$$

The shape of the functions $F_\pm$ and $G_\pm$ depends on the initial conditions for the line charge density and the mean velocity. By imposing the initial conditions we find

$$\begin{aligned} F_-(x) &= \frac{1}{2}\left[\delta\Lambda(x,t=0) + \frac{\Lambda_0}{c_s}\delta V(x,t=0)\right], \\ F_+(x) &= \frac{1}{2}\left[\delta\Lambda(x,t=0) - \frac{\Lambda_0}{c_s}\delta V(x,t=0)\right]. \end{aligned} \tag{42}$$

It is interesting to observe that by choosing appropriate initial conditions we can excite either a forward or a backward wave instead of a combination of the two. For instance, by choosing $\delta V(x,t=0) = -c_s \delta\Lambda(x,t=0)/\Lambda_0$ we excite only the backward wave (slow wave). In this case we obtain

$$\delta V(x,t) = -\frac{c_s}{\Lambda_0}\delta\Lambda(x,t). \tag{43}$$

From the equation (43) one can get the idea of solving the nonlinear system (36) by assuming the existence of a nonlinear algebraic relation between charge line density and mean velocity of the beam, that is, $V = N(\Lambda)$, and substituting this ansatz in the equations (36). Operating in this way we obtain the system of equations:

$$\begin{cases} \dfrac{\partial \Lambda}{\partial t} + \left[N(\Lambda) + \dfrac{dN}{d\Lambda}\Lambda\right]\dfrac{\partial \Lambda}{\partial x} = 0, \\ \dfrac{dN}{d\Lambda}\dfrac{\partial \Lambda}{\partial t} + \left[N(\Lambda)\dfrac{dN}{d\Lambda} + \chi\right]\dfrac{\partial \Lambda}{\partial x} = 0. \end{cases} \tag{44}$$

Since the system (43) is homogeneous in the unknowns $\partial\Lambda/\partial t$ and $\partial\Lambda/\partial x$, a necessary and

sufficient condition for nontrivial solution is that the determinant:

$$\begin{vmatrix} 1 & N+\dfrac{dN}{d\Lambda}\Lambda \\ \dfrac{dN}{d\Lambda} & N\dfrac{dN}{d\Lambda}+\chi \end{vmatrix} = \chi - \left(\frac{dN}{d\Lambda}\right)^2 \Lambda = 0. \tag{45}$$

Therefore we obtain for the unknown function $N(\Lambda)$

$$V = N(\Lambda) = \pm 2\sqrt{\chi\Lambda} + K_0. \tag{46}$$

Now we want to concentrate our attention on the solution that corresponds in the linearized model to a purely backward wave because it is the one that can be reproduced reliably in experiments and PIC simulations. Then we have to choose the determination with the - sign in the relations (46) and $K_0 = 2\sqrt{\chi\Lambda_0}$. Thus we obtain

$$V_+(x,t) = -2\sqrt{\chi\Lambda_+(x,t)} + 2\sqrt{\chi\Lambda_0}. \tag{47}$$

For small density amplitudes equations (47) gives equation (43) to the leading order. To excite this solution we need suitable initial conditions.

Now we can derive the equation for the line density $\Lambda(x,t)$. Substituting (47) in one of the two fluid equations we find the nonlinear first order wave equation:

$$\frac{\partial\Lambda}{\partial t} - c_s(\Lambda)\frac{\partial\Lambda}{\partial x} = 0, \tag{48}$$

where

$$c_s(\Lambda) = c_0\left(3\sqrt{\Lambda/\Lambda_0} - 2\right). \tag{49}$$

The equation (48) has to be solved with the initial condition for the line charge density profile.

To solve equation (48) we can operate as in the following (*e.g.*, [12]). Let us consider the unknown function $\Lambda(x,t)$ in the plane (x,t). Then the expression $\partial\Lambda/\partial t - c_s(\Lambda)(\partial\Lambda/\partial x)$ represents the total derivative of $\Lambda(x,t)$ along a curve C having the slope

$$\frac{dx}{dt} = -c_s(\Lambda). \tag{50}$$

Thus the line charge density remains constant on C. It then follows that $c_s(\Lambda)$ remains constant on C, and therefore the curve C must be a straight line in (x,t) plane with slope $c_s(\Lambda(x,t=0))$ only depending on the initial conditions. Let us assume as initial condition for the charge line density profile $\Lambda(x,t=0) = \Lambda_0 + \Lambda_1 cos(k_0 x)$. Then the solution of the equation (48) is given by

$$\Lambda(x,t) = \Lambda_0 + \Lambda_1 \cos\left[k_0\left(x + c_s(\Lambda(x,t))t\right)\right] \tag{51}$$

Note that (51) gives $\Lambda(x,t)$ implicitly.

The look at this solution makes clear that the density wave moves backwards and with a propagation velocity that is not constant along its whole profile: the higher is the density the faster the wave propagates. That means, a "crest" in the charge density moves quicker to the left than a "valley", and furthermore the peak of the crest comes to be faster than any other region along the ring. Such a difference in the propagation velocity results in a distortion of the initial shape into a

typical wave-breaking profile. Any compressive part of the wave, where the propagation velocity is a decreasing function of x ultimately "breaks" to give triple-valued solution for the line charge density.

For a given set of beam and machine parameters, the predictions of this model is compared to the simulated density profiles resulting from the PIC (particle-in-cell) code PATRIC (a beam current of 0.366 mA has been considered). Care must be taken, in this case, in the assignment of the initial conditions: as a matter of fact, if we start with zero average velocity and sinusoidal line density, we must expect to find both the forward and the backward wave running across the beam and the beam evolution does not verify equation (51). That's why we should work out a situation where the initial conditions are such as to verify equation (47). This situation might be achieved by letting an instability to grow through its linear phase first and then turning off the source of the instability itself, leaving the only space charge impedance still acting on the beam. In this way we can create initial conditions that excite only the slow wave, since the fast one will be damped so far as the evolution we are interested in starts, and hence verify, even if only approximately, equation (47). The line density profiles relative to such a beam simulation, after the resistive part of the impedance has been switched off, are shown in Figure 9a. The slow wave keeps moving backwards (the frequency shift only slightly changes) and, within some 40 ms, gets steep on the left side with no further increasing of its amplitude; later on the wave breaks down. The solution (50) of the cold fluid model also shows this steepening tendency of the slow wave, as we can see in Figure 9b. Afterwards the line density becomes a three-values function and our description gets consequently not physically meaningful any longer because when there are high spatial gradients the term $\partial \Pi / \partial s$ in equation (24) cannot be neglected even in the limit case $\Pi \to 0$. Anyhow, the agreement during the phase of the steepening seems to suggest that this phenomenon, which we have clearly observed late in the instability development both in measurements at the ESR and in the relative PIC simulations, is simply a fluid mechanism that doesn't depend on the actual beam distribution in the longitudinal phase space. It is the nonlinear terms in the fluid equations that cause a non uniform frequency shift along the beam with consequent waveform distortion and steepening in the direction of the travelling wave.

Now a question arises about the role of the space charge in the steepening mechanism. The space charge is fundamental, the steepening does not occur if its effects are absent. We have seen this by PIC simulations in which the effects of the space charge were artificially switched off. Why is the space charge so important? When the beam is space charge dominated the dispersion relation for the waves is almost linear. In this situation the high order harmonic generated by the convective terms are at all times in resonance with the fundamental one. This causes their amplitudes to grow in time. The appearance of these high order harmonics is responsible for the steepening. This is the mechanism of resonant wave-wave interaction well known in gas dynamics [12] and plasma physics [13].

6. Conclusions and outlook

We have seen that a cold nonlinear fluid model might be used to explain or to predict the beam dynamics (the more successfully the farther we are from the stability boundary - little Landau damping effects from momentum spread) not only in the linear phase of the evolution but also later. In particular we have proved that the wave steepening observed in the beam evolution during an instability is only a fluid effect due to the nonlinear convective terms present in the equations.

Their influence is obvious if we also notice that in a space charge dominated beam there is generation of higher order harmonics, which soon become resonant due to wave-wave interaction. Instability growth saturation needs to be investigated with a more detailed model. Such a model could be set up by taking into account some of the effects we chose to ignore so far (like, for instance, the term of pressure, which contains somehow information about the beam momentum spread) and by closing the system with assumptions "ad hoc" (constitutive relations). The results collected herein show anyway the reliability of this way of description of the beam.

References

[1] I. Hofmann, Fus. Engin. and Design, **32-33**, 33 (1996).

[2] A.G. Ruggiero and V.G. Vaccaro, CERN-Report ISR-TH/68-33, CERN, Geneva (1968).

[3] M.Q. Barton, C.E. Nielsen, *Longitudinal Instability and cluster formation in the Cosmotron*, International Conference on high energy accelerators, Brookhaven, September 1961.

[4] J. E. Keil and E. Messerschmid, Nucl. Instrum. Methods **128**, 203 (1975).

[5] Y. Chin and K. Yokoya, Phys. Rev. D **28**, 2141 (1983).

[6] S. Bogacz and K.-Y. Ng, Phys. Rev. D **36**, 1538 (1987).

[7] J. Bisognano, I. Haber, L. Smith, A. Sterlieb, IEEE Trans. on Nuclear Science, NS-28, 2512-2514, 1981.

[8] J. Bisognano, Solitary waves in particle beams, **EPAC** Barcellona, (1996).

[9] G. Rumolo, I. Hofmann, G. Miano, U. Oeftiger, *Comparison between theory and simulations for longitudinal instabilities of coasting beams* , to be published on Nucl. Instrum. Methods .

[10] G.Rumolo, U. Oeftiger, I. Hofmann, R.C. Baer, K. Beckert, M. Steck, *Measurement and interpretation of longitudinal instabilities in the ESR* , to be published on Nucl. Instrum. Methods.

[11] M. Reiser, Theory and design of charged particle beams, John Wiley & Sons, New York, (1994).

[12] G. B. Whitham, Linear and nonlinear waves, John Wiley&Sons New York, (1974).

[13] A. A. Galeev and R. S. Sagdeev, *Nonlinear plasma theory* in *Reviews of Plasma Physics* edited by Acad. M. A. Leontovich, Vol. 7 (1979).

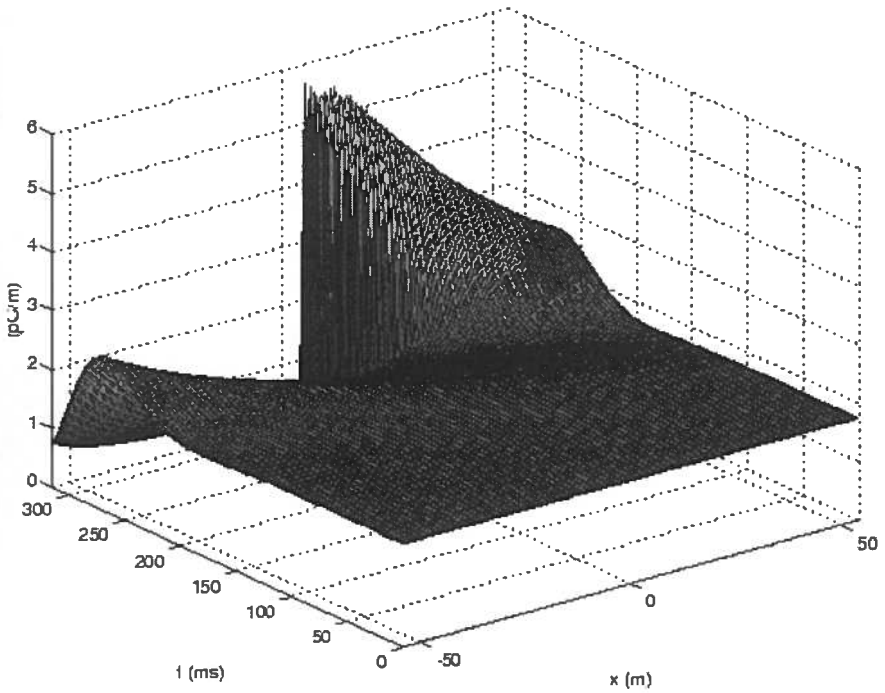

Fig. 1 – Space-time evolution of the line charge density $\Lambda(x,t)$ obtained by using the cold fluid model for $\Delta f = -17.4\ kHz$, and $I_0 = 0.366$ mA.

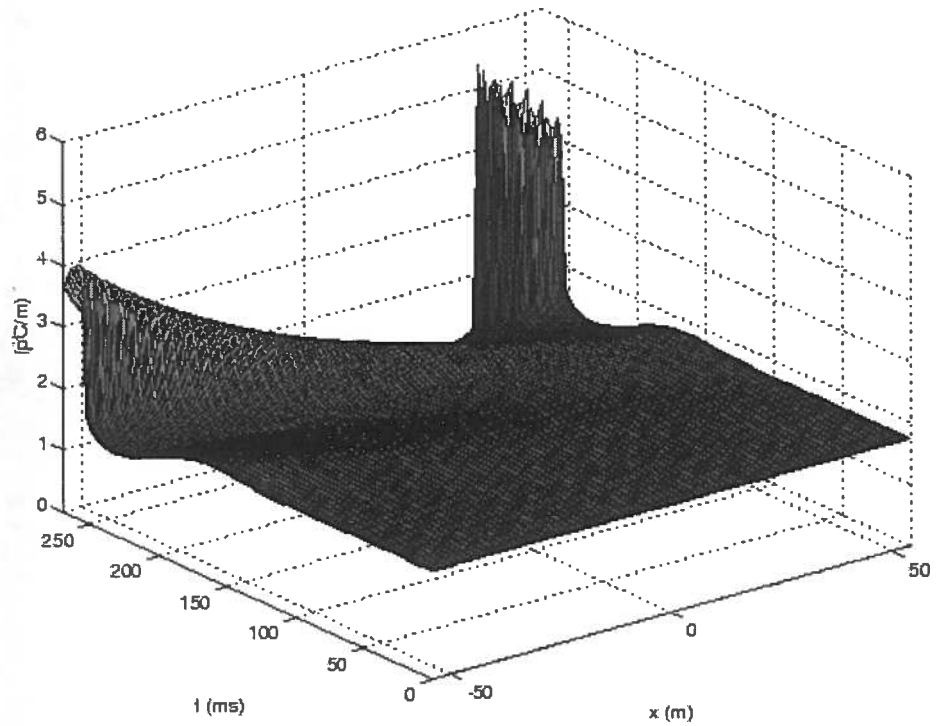

Fig. 2 – Space-time evolution of the line charge density $\Lambda(x,t)$ obtained by using the cold fluid model for $\Delta f = 0$, and $I_0 = 0.366$ mA.

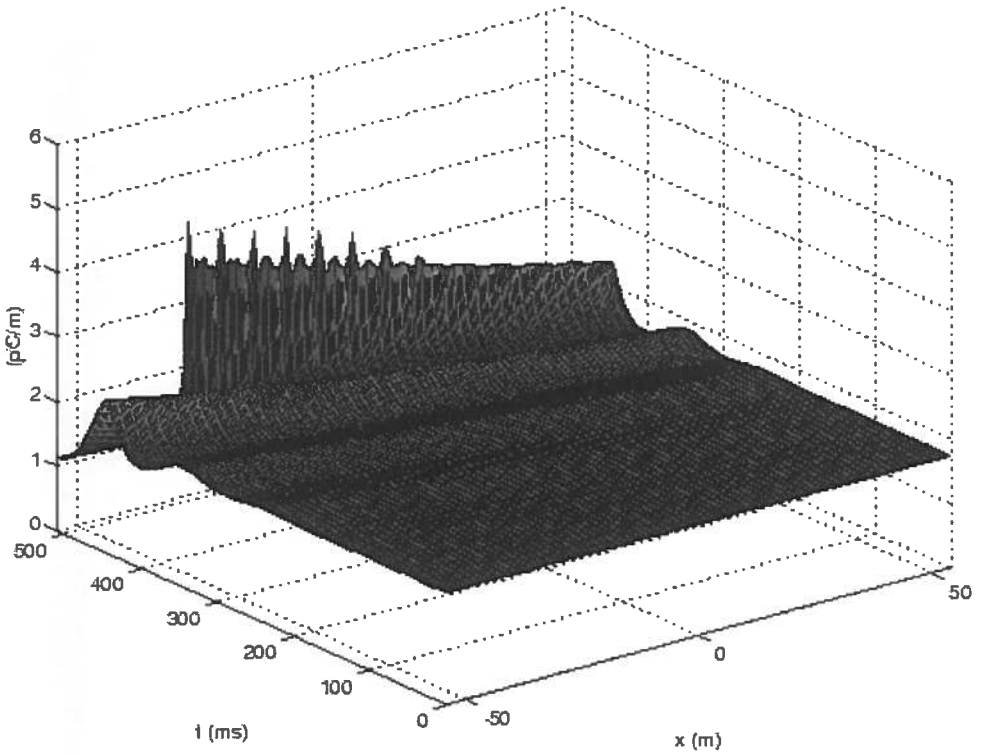

Fig. 3 – Space-time evolution of the line charge density $\Lambda(x,t)$ obtained by using the cold fluid model for $\Delta f = 16.4\ kHz$, and $I_0 = 0.366$ mA.

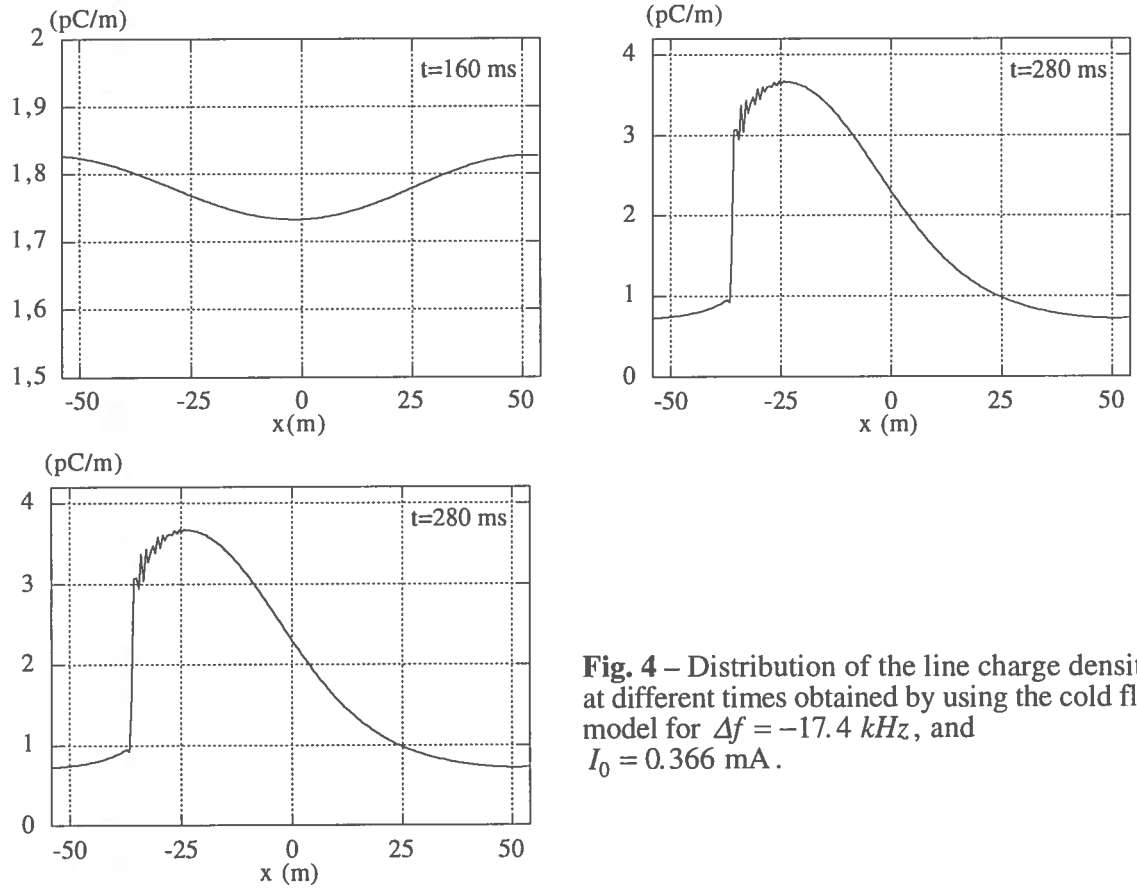

Fig. 4 – Distribution of the line charge density at different times obtained by using the cold fluid model for $\Delta f = -17.4\ kHz$, and $I_0 = 0.366$ mA.

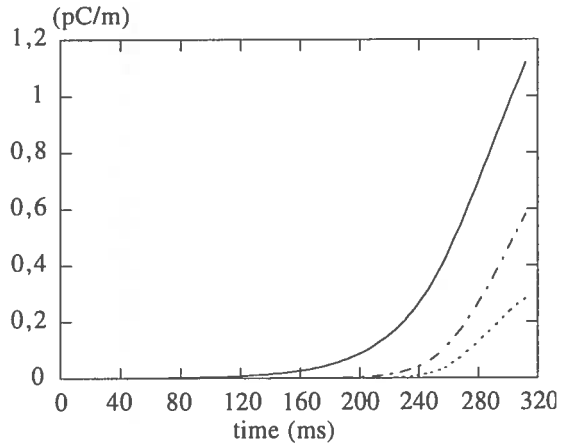

Fig. 5 –Time evolution of the first (——), second (–·–·–) and third (·····) spatial harmonics of the line charge density obtained by using the cold fluid model for $\Delta f = -17.4\ kHz$, and $I_0 = 0.366$ mA.

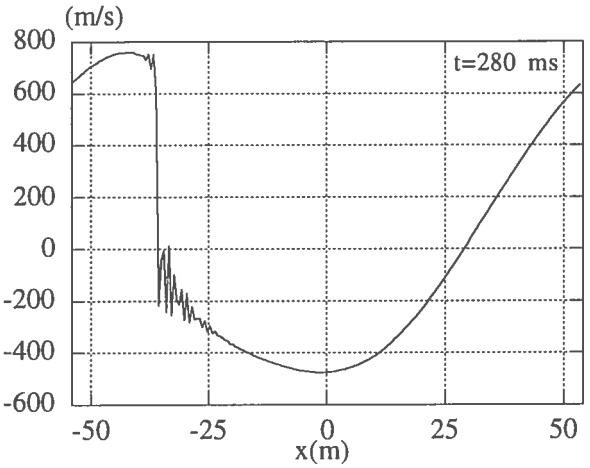

Fig. 6 – Distribution of the mean velocity obtained by using the cold fluid model for $\Delta f = -17.4\ kHz$, and $I_0 = 0.366$ mA.

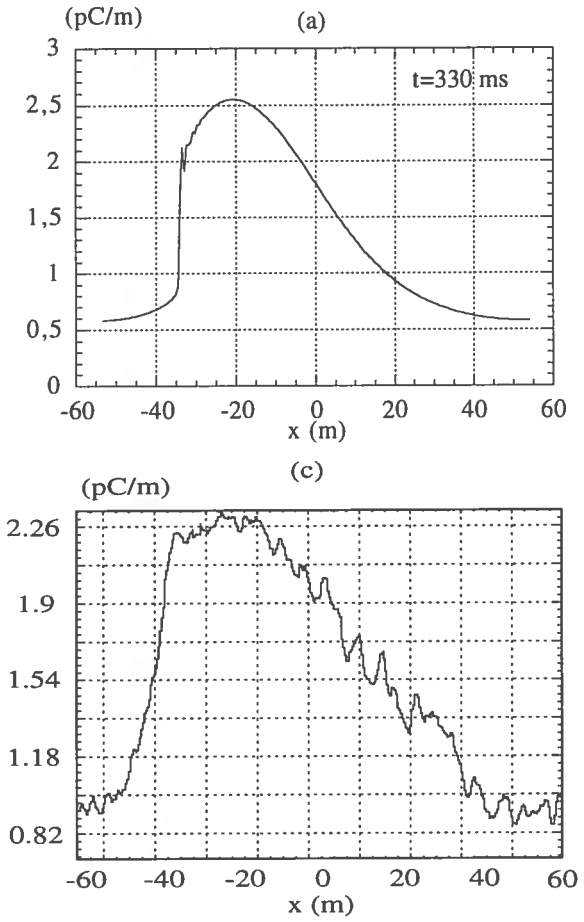

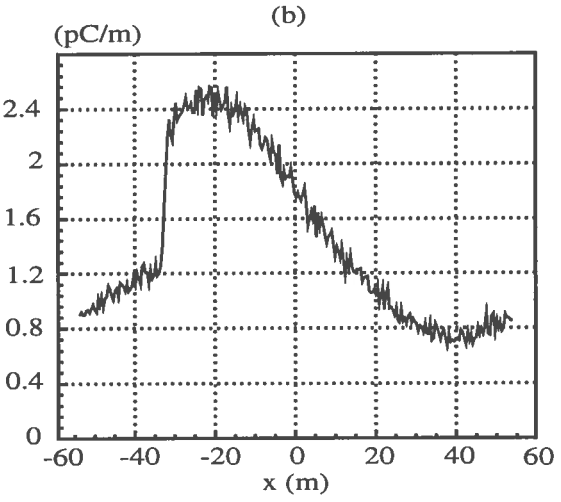

Fig. 7 – Distribution of the line charge density at t=330 ms for $\Delta f = -17.4\ kHz$ and $I_0 = 0.276\ mA$:
(a) cold fluid model;
(b) particle-in-cell simulation (PATRIC code);
(c) ESR measurements.

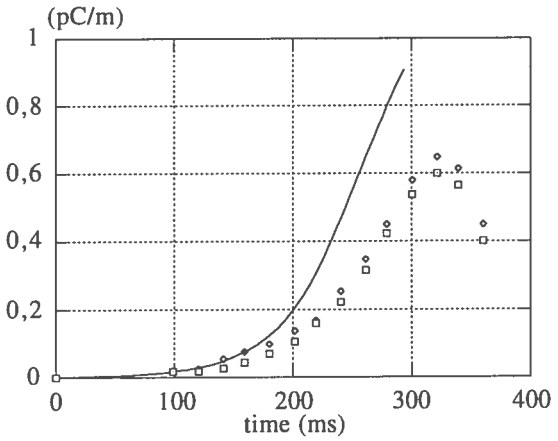

Fig. 8 – Time evolution of the first spatial harmonic of the line charge density for $\Delta f = -17.4\ kHz$ and $I_0 = 0.276\ mA$: —— cold fluid model, ESR measurements (□) and particle-in-cell simulation with PATRIC code (◇).

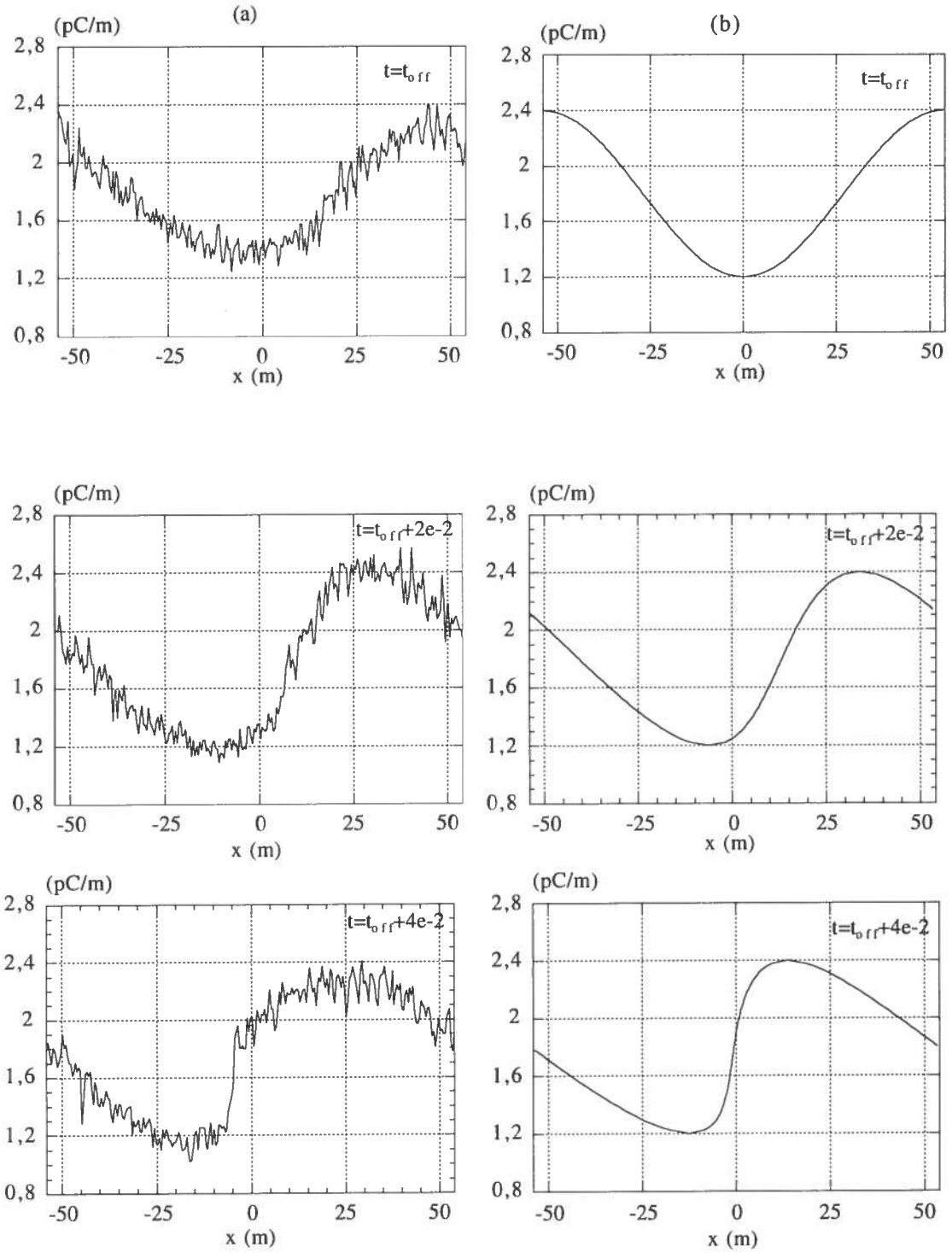

Fig. 9 – Distribution of the line charge density at different times for a purely space charge impedance, and $I_0 = 0.366$ mA: (a) particle-in-cell simulation (PATRIC code); (b) analytical solution of the cold fluid model.